

## Photochemistry of Formaldoxime–Nitrous Acid Complexes in an Argon Matrix: Identification of Formaldoxime Nitrite

Barbara Golec, Andrzej Bil, and Zofia Mielke\*

Faculty of Chemistry, University of Wrocław, Joliot-Curie 14, 50-383 Wrocław, Poland

Received: May 24, 2009; Revised Manuscript Received: July 10, 2009

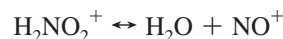
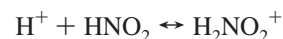
We have studied the structure and photochemistry of the formaldoxime–nitrous acid system ( $\text{CH}_2\text{NOH}-\text{HONO}$ ) by help of FTIR matrix isolation spectroscopy and ab initio methods. The MP2/6-311++G(2d,2p) calculations show stability of six isomeric  $\text{CH}_2\text{NOH}\cdots\text{HONO}$  complexes. The FTIR spectra evidence formation of two hydrogen bonded complexes in an argon matrix whose structures are determined by comparison of the experimental spectra with the calculated ones for the six stable complexes. In the matrix there is present the most stable cyclic complex with two  $\text{O}-\text{H}\cdots\text{N}$  bonds; a strong bond is formed between the OH group of HONO and the N atom of  $\text{CH}_2\text{NOH}$  and the weaker one between the OH group of  $\text{CH}_2\text{NOH}$  and the N atom of HONO. In the other complex present in the matrix the OH group of formaldoxime is attached to the OH group of HONO forming an  $\text{O}-\text{H}\cdots\text{O}$  bond. The irradiation of the  $\text{CH}_2\text{NOH}\cdots\text{HONO}$  complexes with the filtered output of the mercury lamp ( $\lambda > 345$  nm) leads to the formation of formaldoxime nitrite,  $\text{CH}_2\text{NONO}$ , and its two isomeric complexes with water. The main product is the  $\text{CH}_2\text{NONO}\cdots\text{H}_2\text{O}$  complex in which water is hydrogen bonded to the N atom of the  $\text{C}=\text{N}$  group. The identity of the photoproducts is confirmed by both FTIR spectroscopy and MP2 or QCISD(full) calculations with the 6-311++G(2d,2p) basis set. The intermediate in this reaction is iminoxyl radical that is formed by abstraction of hydrogen atom from formaldoxime OH group by an OH radical originating from HONO photolysis.

### Introduction

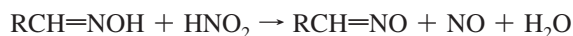
The oxidation of oximes with nitrous acid in solutions is a long known procedure for the recovery of aldehydes and ketones from the parent oximes.<sup>1,2</sup> Although the mechanism of the reaction was studied very extensively prior to the 1990s<sup>3,4</sup> its stoichiometry is still not well-defined and the nature of intermediates is only partly understood. The recent, growing interest in regeneration of carbonyl compounds from stable and readily prepared oximes<sup>5–9</sup> is due to increasing synthetic importance of this method for carbonyls production. It is desirable to develop a method that is environmentally benign and can be applied to a wide range of aldoximes and ketoximes with high selectivity and easy product isolation. In this respect, the photochemical production of carbonyl compounds from oximes has also been explored.<sup>8,9</sup> It was reported recently that singlet oxygen generated by photosensitization reacts with aldoximes and ketoximes to produce their corresponding carbonyl compounds.<sup>8</sup> Reasonably good yields of carbonyl compounds from the oximes were obtained through the use of a photosensitized electron-transfer reaction.<sup>9</sup>

Oximes are usually smoothly degraded to ketones by nitrous acid in the presence of mineral acid. However, when the site of the oxime is sterically hindered, nitrogen containing compounds may be isolated.<sup>3,4</sup> The structures of these compounds, that are intermediates in the oxidation reaction of oximes, and the mechanisms of their formation have been the subject of long, vigorous discussion without universal agreement being reached. One of the postulated reaction intermediates at that time was oxime nitrite,  $>\text{C}=\text{N}-\text{O}-\text{N}=\text{O}$ ; however, according to our knowledge, no oxime nitrite has been characterized so far.

The reaction of oximes with nitrous acid is usually conducted in the presence of an excess of mineral acid. Kliegman and Barnes<sup>3</sup> studied the reaction of butyraldoxime with nitrous acid in the presence of excess and without excess of mineral acid. On the basis of the products distribution the authors concluded that the mechanism of the reaction is different in the two cases. In the presence of mineral acid a rapid reaction takes place to give the nitrosonium ion, and it is  $\text{NO}^+$  which is an oxidizing agent:



On the other hand, when there is no excess acid present, it is nitrous acid which is reacting with butyraldoxime to give the iminoxyl radical, NO and water.



The iminoxyl radical,  $\text{RCH}=\text{NO}$ , was also proposed as an intermediate product of the reaction of oximes with such oxidizing agents as ceric ion, palladium(IV) acetate, lead tetraacetate and  $\text{NO}_2$ .<sup>3</sup> It has been suggested recently that iminoxyl radical is an intermediate in deprotection of oximes to their corresponding carbonyl compounds through the use of photosensitized electron-transfer reactions.<sup>9</sup>

In this paper we report the study of the photoinduced reaction between the simplest oxime, which is formaldoxime, and nitrous acid in solid argon. The photoproducts of the reaction are water and formaldoxime nitrite that is identified for the first time. The

\* Corresponding author. E-mail: zm@wchuwr.pl.

formation of formaldoxime nitrite evidence that iminoxyl radical is an intermediate in this reaction.

## Experimental and Computational Methods

**Infrared Matrix Isolation Studies.** Formaldoxime and HONO were obtained in the same way as previously described.<sup>10–13</sup> Crystalline ammonium nitrite ( $\text{NH}_4\text{NO}_2$ ) was used as a source of gaseous HONO, and  $\text{ND}_4\text{NO}_2$  was used as a source of DONO. Formaldoxime,  $\text{CH}_2\text{NOH}$ , was generated from formaldoxime trimer hydrochloride salt (Aldrich, >98%). HONO,  $\text{CH}_2\text{NOH}$  and Ar were deposited simultaneously onto a gold-plated copper mirror held at 17 K by a closed cycle helium refrigerator (Air Products, Displex 202A). No exact matrix ratio could be determined, but the concentration of the  $\text{CH}_2\text{NOH}/\text{HONO}/\text{Ar}$  mixture was varied by changing the flow rate of argon gas and the temperatures of the solids. After the infrared spectra of the initial deposit had been recorded, the sample was subjected to the filtered radiation of a 200 W medium pressure mercury lamp (Phillipps CS200W2). A 10 cm water filter served to reduce the amount of infrared radiation reaching the matrix; a glass long-wavelength pass filter (Zeiss WG345) was applied to cut off the radiation with  $\lambda < 345$  nm. The spectra were registered after 10, 30, 60, and 120 min of matrix irradiation. After the irradiation process was completed, the samples were annealed to 30 K for 15 min and recooled to 11 K, and the spectra of annealed matrices were recorded. The infrared spectra (resolution  $0.5\text{ cm}^{-1}$ ) were recorded in a reflection mode with a Bruker 113v FTIR spectrometer using a MCT detector cooled by liquid  $\text{N}_2$ .

**Computational Methods.** Optimization of all the structures as well as calculation of harmonic vibrational spectra were performed with the Gaussian03 suite of programs.<sup>14</sup> All-electron MP2/6-311++G(2d,2p) calculations<sup>15,16</sup> were done to optimize the structures and to calculate the energies and harmonic frequencies of all considered species. The QCISD(full)/6-311++G(2d,2p) method<sup>17,18</sup> was used to optimize the structure of formaldoxime nitrite and its complexes as well as to calculate its harmonic spectrum. Interaction energies were corrected by the Boys–Bernardi full counterpoise procedure.<sup>19</sup> The calculated frequencies were used to account for the zero-point vibrational energy contribution.

## Results and Discussion

**Formaldoxime–Nitrous Acid Complexes.** The ab initio calculations show six true minima on the potential energy surface of the  $\text{CH}_2\text{NOH}$ –*trans*-HONO system, and the corresponding structures are depicted in Figure 1. The interaction energies of the six complexes are also presented in Figure 1. The global minimum corresponds to a planar, hydrogen-bonded complex,  $\text{I}_{\text{HF}}$ , in which the OH group of nitrous acid is attached to the nitrogen atom of formaldoxime forming a strong  $\text{O}-\text{H}\cdots\text{N}$  bond. The calculated parameters suggest an additional weak  $\text{O}-\text{H}\cdots\text{N}$  bond in this complex between the OH group of formaldoxime and the nitrogen atom of the acid. The lack of the weak  $\text{O}-\text{H}\cdots\text{N}$  bond in the  $\text{II}_{\text{HF}}$  complex leads to a decrease of the interaction energy by ca.  $5\text{ kJ mol}^{-1}$  (from  $27.54\text{ kJ mol}^{-1}$  to  $22.45\text{ kJ mol}^{-1}$ ) in this complex as compared to the  $\text{I}_{\text{HF}}$  one. The other four isomeric structures are nonplanar. In the complexes  $\text{III}_{\text{HF}}$  and  $\text{IV}_{\text{HF}}$  that exhibit similar stability ( $17.18$  and  $16.81\text{ kJ mol}^{-1}$ , respectively), the  $\text{O}-\text{H}\cdots\text{O}$  hydrogen bonds between the OH group of HONO and the oxygen atom of formaldoxime are formed, however the electrostatic forces probably play an important role in the stabilization of these two complexes. In the complex  $\text{V}_{\text{HF}}$  the OH group

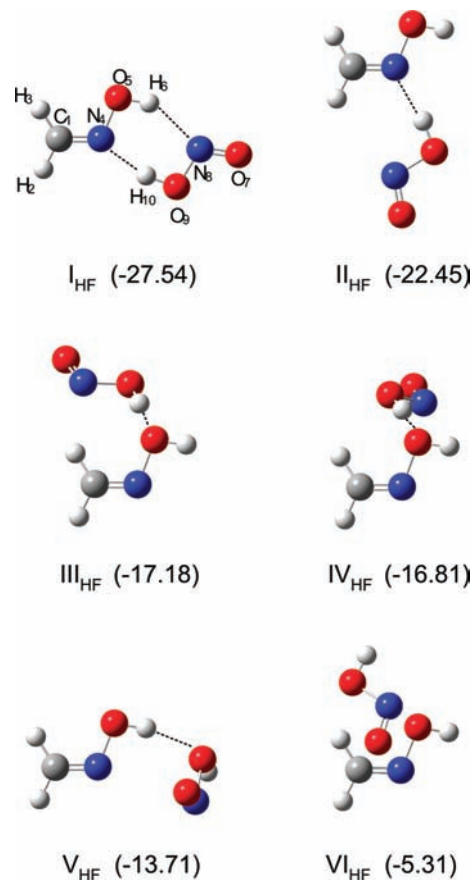


**Figure 1.** The structures of the  $\text{CH}_2\text{NOH}$ –HONO system optimized at the MP2/6-311++G(2d, 2p) level. In the parentheses the interaction energies ( $E^{\text{CP}}(\text{ZPE})$ ) are given ( $\text{kJ mol}^{-1}$ ).

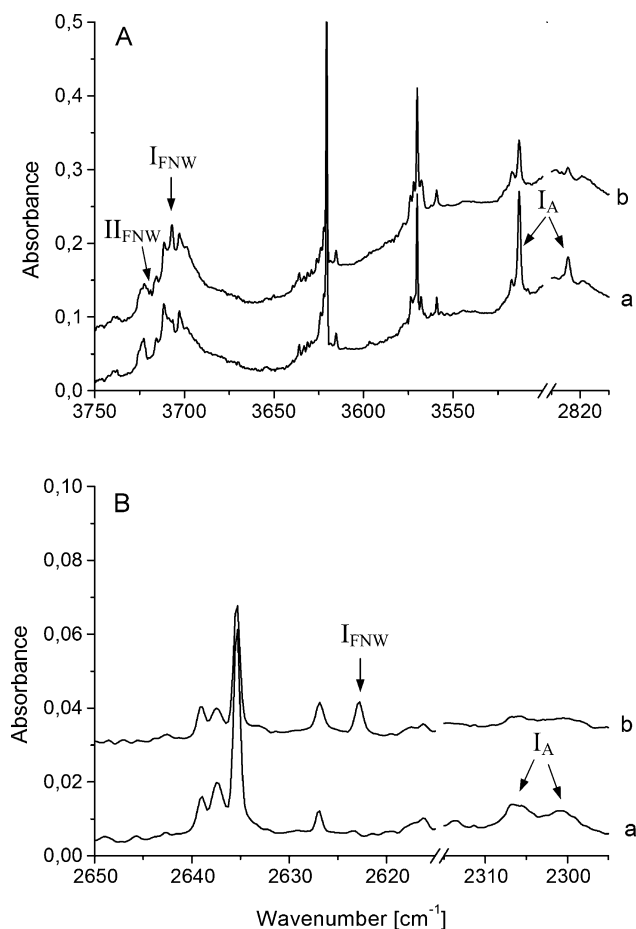
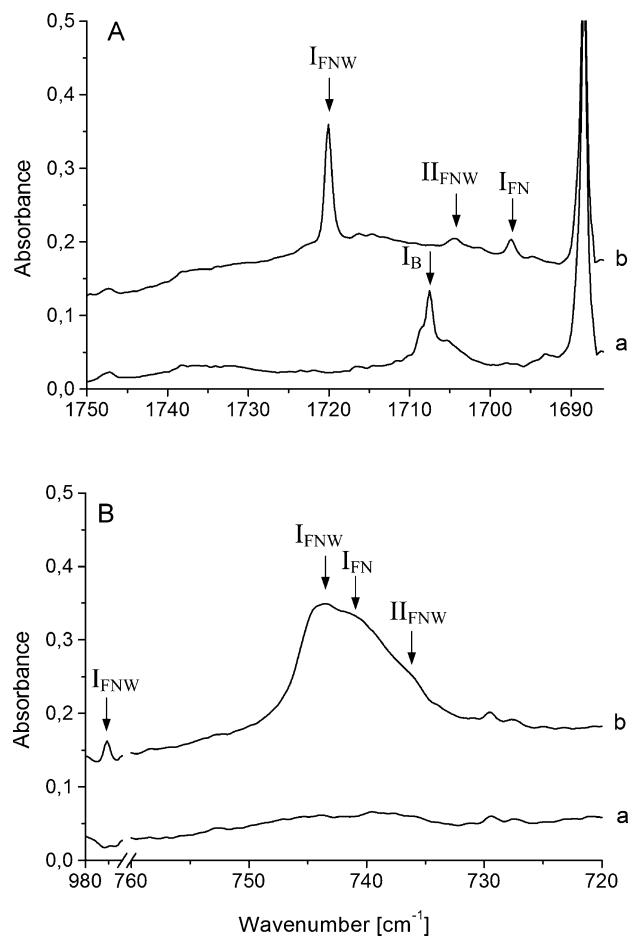
of formaldoxime serves as a proton donor toward the oxygen atom of nitrous acid OH group forming relatively strong  $\text{O}-\text{H}\cdots\text{O}$  bond. The  $\text{V}_{\text{HF}}$  complex is ca.  $3\text{ kJ mol}^{-1}$  less stable than the  $\text{III}_{\text{HF}}$  and  $\text{IV}_{\text{HF}}$  ones and is ca.  $8.5\text{ kJ mol}^{-1}$  more stable than the less stable non-hydrogen bonded complex  $\text{VI}_{\text{HF}}$ . In Table 1 the selected parameters describing the  $\text{I}_{\text{HF}}$  and  $\text{V}_{\text{HF}}$  complexes (that are present in the studied matrices as discussed below) are collected; the structural parameters of all optimized structures and their harmonic frequencies are collected in Tables 1 and 2 in the Supporting Information.

The selected regions of the infrared spectra of the argon matrices doped with formaldoxime and nitrous acid are shown in Figures 2 and 3. A set of new bands appear in the spectra of  $\text{CH}_2\text{NOH}/\text{HONO}/\text{Ar}$  matrix that are not observed in earlier reported spectra of  $\text{CH}_2\text{NOH}/\text{Ar}$  and  $\text{HONO}/\text{Ar}$  matrices.<sup>11,12</sup> The bands can be separated into two groups taking as a criterion their behavior during matrix irradiation. The intensities of the bands belonging to the group  $\text{I}_B$  (see Figure 3A) decrease more quickly when the matrix is subjected to filtered ( $\lambda > 345$  nm) or unfiltered radiation of Hg lamp than those belonging to the  $\text{I}_A$  group (see Figure 2). The  $\text{I}_B$  bands disappear after ca. 30 min whereas the  $\text{I}_A$  bands are still visible even after 2 h of matrix irradiation. The counterparts of the  $\text{I}_A$  and  $\text{I}_B$  bands observed in  $\text{CH}_2\text{NOH}/\text{HONO}/\text{Ar}$  experiments were identified in the spectra of  $\text{CH}_2\text{NOH}/\text{DONO}/\text{Ar}$  matrices.

The frequencies of all bands assigned to groups  $\text{I}_A$  and  $\text{I}_B$  in HONO and DONO experiments are collected, respectively, in Tables 2 and 3. Four  $\text{I}_A$  bands appear in the regions of the  $\nu(\text{OH})$ ,  $\delta(\text{NOH})$ ,  $\nu(\text{NO})$  and  $\tau(\text{OH})$  *trans*-HONO vibrations (Table 2). The other identified  $\text{I}_A$  bands occur in the proximity

**TABLE 1:** Selected Parameters Describing the CH<sub>2</sub>NOH and HONO Monomers (M) and the I<sub>HF</sub>, V<sub>HF</sub> Structures of the CH<sub>2</sub>NOH–*trans*-HONO Complex (Labeling Refers to Figure 1)<sup>a</sup>

parameter	M	I <sub>HF</sub>	V <sub>HF</sub>
<i>r</i> C <sub>1</sub> –H <sub>2</sub>	1.077	1.077	1.077
<i>r</i> C <sub>1</sub> –H <sub>3</sub>	1.083	1.082	1.083
<i>r</i> C <sub>1</sub> –N <sub>4</sub>	1.278	1.277	1.279
<i>r</i> N <sub>4</sub> –O <sub>5</sub>	1.409	1.394	1.400
<i>r</i> O <sub>5</sub> –H <sub>6</sub>	0.961	0.969	0.968
<i>r</i> O <sub>7</sub> –N <sub>8</sub>	1.178	1.193	1.162
<i>r</i> N <sub>8</sub> –O <sub>9</sub>	1.439	1.382	1.509
<i>r</i> O <sub>9</sub> –H <sub>10</sub>	0.967	0.989	0.968
<i>R</i> H <sub>6</sub> ···N <sub>8</sub>		2.126	
<i>R</i> H <sub>10</sub> ···N <sub>4</sub>		1.816	
<i>R</i> H <sub>6</sub> ···O <sub>9</sub>			1.938
<i>θ</i> C <sub>1</sub> –N <sub>4</sub> –O <sub>5</sub>	110.5	112.3	111.2
<i>θ</i> N <sub>4</sub> –O <sub>5</sub> –H <sub>6</sub>	102.2	102.4	101.7
<i>θ</i> O <sub>7</sub> –N <sub>8</sub> –O <sub>9</sub>	110.9	112.8	110.4
<i>θ</i> N <sub>8</sub> –O <sub>9</sub> –H <sub>10</sub>	101.4	100.8	100.8
<i>θ</i> O <sub>5</sub> –H <sub>6</sub> –N <sub>8</sub>		146.3	
<i>θ</i> O <sub>5</sub> –H <sub>6</sub> –O <sub>9</sub>			159.9
<i>θ</i> O <sub>9</sub> –H <sub>10</sub> –N <sub>4</sub>		159.9	
<i>φ</i> N <sub>4</sub> –O <sub>5</sub> –H <sub>6</sub> –N <sub>8</sub>		0.0	
<i>φ</i> N <sub>8</sub> –O <sub>9</sub> –H <sub>10</sub> –N <sub>4</sub>		0.0	
<i>φ</i> N <sub>4</sub> –O <sub>5</sub> –H <sub>6</sub> –O <sub>9</sub>			1.7

<sup>a</sup> Distances are in Å and angles in deg.**Figure 2.** (A) The spectra of the CH<sub>2</sub>NOH/HONO/Ar matrix in the  $\nu(\text{OH})$  region and (B) the spectra of the CH<sub>2</sub>NOH/DONO/Ar matrix in the  $\nu(\text{OD})$  region; (a) the spectra recorded after matrix deposition and (b) the spectra recorded after the matrix was subjected to  $\lambda > 345$  nm radiation for 120 min. The bands due to the CH<sub>2</sub>NOH···HONO complexes are marked by I<sub>A</sub> and those due to the photoproducts by I<sub>FNW</sub> and II<sub>FNW</sub>.**Figure 3.** The spectra of the CH<sub>2</sub>NOH/HONO/Ar matrix in the 1750–1680 cm<sup>-1</sup> region (A) and in the 980–720 cm<sup>-1</sup> region (B); (a) the spectra recorded after matrix deposition and (b) the spectra recorded after the matrix was subjected to  $\lambda > 345$  nm radiation for 120 min. The band due to the CH<sub>2</sub>NOH···HONO complex is marked by I<sub>B</sub> and the bands due to photoproducts by I<sub>FN</sub>, I<sub>FNW</sub> and II<sub>FNW</sub>.

of the formaldoxime monomer bands. Among five identified I<sub>B</sub> absorptions two occur in the regions of the  $\nu(\text{N}=\text{O})$  and  $\delta(\text{NOH})$  *trans*-HONO vibrations, and the other three in the vicinity of the formaldoxime vibrations (Table 3). The two groups of bands, I<sub>A</sub> and I<sub>B</sub>, are assigned with confidence to two types of the CH<sub>2</sub>NOH···*trans*-HONO complexes. No band could be assigned to the complexes formed by the *cis*-HONO isomer. The lack of observation of the complexes of *cis*-HONO isomer is due to its small concentration in the matrix.<sup>12</sup> In earlier reported spectra of HONO complexes with various bases, only one or two of the most intense bands of bonded *cis*-HONO were identified.<sup>13,20</sup>

The I<sub>A</sub> bands due to the perturbed *trans*-HONO vibrations have frequencies close to those observed for the *trans*-HONO complex with ammonia.<sup>12</sup> The characteristic feature of the two complexes, CH<sub>2</sub>NOH···*trans*-HONO and NH<sub>3</sub>···*trans*-HONO, is very strong perturbation of the NOH group vibrations. The OH stretch is ca. 750, 820 cm<sup>-1</sup> red-shifted and the NOH bend is ca. 158, 180 cm<sup>-1</sup> blue-shifted, respectively, in the complexes with formaldoxime and ammonia. This indicates that in the formaldoxime complex, as in the ammonia one, the *trans*-HONO molecule acts as a proton donor toward the nitrogen atom of CH<sub>2</sub>NOH forming a very strong O–H···N hydrogen bond. As discussed earlier, the calculations indicate that the two most stable structures, I<sub>HF</sub> and II<sub>HF</sub>, are stabilized by the O–H···N bond between the OH group of HONO and the N atom of

**TABLE 2: The Observed ( $I_A$ ) and MP2/6-311++G(2d,2p) Calculated (M) Frequencies ( $\text{cm}^{-1}$ ) and Frequency Shifts ( $\Delta\nu = \nu_{\text{comp}} - \nu_{\text{mon}}$ ) for the  $\text{CH}_2\text{NOH}$ , HONO and DONO Monomers (M) and Their  $I_{\text{HF}}$  and  $II_{\text{HF}}$  Complexes**

approx description	$\text{CH}_2\text{NOH} \cdots \text{trans-HONO}$						$\text{CH}_2\text{NOH} \cdots \text{trans-DONO}$					
	exptl			calcd			exptl			calcd		
	M	$I_A$		M	$I_{\text{HF}}$	$II_{\text{HF}}$	M	$I_A$		M	$I_{\text{HF}}$	
	$\nu_{\text{exp}}$	$\nu_{\text{exp}}$	$\Delta\nu_{\text{exp}}$	$\nu_{\text{calc}}$	$\Delta\nu_{\text{calc}}$	$\Delta\nu_{\text{calc}}$	$\nu_{\text{exp}}$	$\nu_{\text{exp}}$	$\Delta\nu_{\text{exp}}$	$\nu_{\text{calc}}$	$\Delta\nu_{\text{calc}}$	
	$\text{CH}_2\text{NOH}$											
$\nu(\text{OH})$	3620.7	3513.2	-107	3861	-145	-12	3620.7	3513.4	-107	3861	-146	
$\nu(\text{C}=\text{N})$	1636.6	1666.9	+20	1667	+20	+3	1636.6	1666.7	+30	1667	+19	
$\delta(\text{CH}_2)$	1408.3	1440.6	+34	1468	+35	+8	1408.3	1437.2	+29	1468	+33	
		1443.7										
$\delta(\text{NOH})$	1314.2	1358.8	+44	1348	+53	+12	1314.2	1357.5	+43	1348	+54	
		1357.1										
$\omega(\text{CH}_2)$	953.1	970.1	+18	974	+12	+26	953.1	972.8	+20	974	+11	
		972.9										
$\nu(\text{N}-\text{O})$	886.4	909.9	+27	914	+32	+29	886.4			914	+32	
	880.2						880.2					
$\tau(\text{NOH})$	400			402	+184	-31	400			402	+178	
	<i>trans-HONO</i>						<i>trans-DONO</i>					
$\nu(\text{OH})/\nu(\text{OD})$	3572.1	2823.3	-747	3789	-456	-234	2635.0	2306.2	-333	2759	-327	
	3568.1						2638.1	2301.4				
$\nu(\text{N}=\text{O})$	1689.1			1644	0	-10	1682.6			1633	-46	
	1688.0						1681.6					
$\delta(\text{NOH})/\delta(\text{NOD})$	1265.8	1423.8	+159	1291	+179	+128	1013.9	1013.1	+100	1022	+128	
	1263.9						1011.4					
$\nu(\text{N}-\text{O})$	800.4	871.4	+73	794	+132	+94	748.9	872.2	+126	741	+160	
	796.6						744.3					
$\delta(\text{ONO})$	608.7			583	+120	+107	602.4			576	+111	
							601.5					
$\tau(\text{OH})/\tau(\text{OD})$	549.4	844.3	+323	582	+373	+251				440	+261	
	548.2											

**TABLE 3: The Observed ( $I_B$ ) and MP2/6-311++G(2d,2p) Calculated ( $V_{\text{HF}}$ ) Frequencies ( $\text{cm}^{-1}$ ) and Frequency Shifts ( $\Delta\nu = \nu_{\text{comp}} - \nu_{\text{mon}}$ ) for the  $\text{CH}_2\text{NOH}$ , HONO and DONO Monomers (M) and Their Complexes**

approxim description	$\text{CH}_2\text{NOH} \cdots \text{trans-HONO}$						$\text{CH}_2\text{NOH} \cdots \text{trans-DONO}$					
	exptl			calcd			exptl			calcd		
	M	$I_B$		M	$V_{\text{HF}}$		M	$I_B$		M	$V_{\text{HF}}$	
	$\nu_{\text{exp}}$	$\nu_{\text{exp}}$	$\Delta\nu_{\text{exp}}$	$\nu_{\text{calc}}$	$\Delta\nu_{\text{calc}}$		$\nu_{\text{exp}}$	$\nu_{\text{exp}}$	$\Delta\nu_{\text{exp}}$	$\nu_{\text{calc}}$	$\Delta\nu_{\text{calc}}$	
	$\text{CH}_2\text{NOH}$											
$\nu(\text{OH})$	3620.7			3861	-144		3620.7			3861	-145	
$\nu(\text{C}=\text{N})$	1636.6			1667	+3		1636.6			1667	+3	
$\delta(\text{CH}_2)$	1408.3			1468	+26		1408.3			1468	+26	
$\delta(\text{NOH})$	1314.2	1345.7	+32	1348	+43		1314.2			1348	+43	
$\omega(\text{CH}_2)$	953.1			974	-5		953.1			974	-4	
$\nu(\text{N}-\text{O})$	886.4	901.2	+18	914	+16		886.4	901.9	+19	914	+16	
	880.2						880.2					
$\tau(\text{NOH})$	400.0	647.0	+247	402	+295		400.0				+286	
										402.0		
	<i>trans-HONO</i>						<i>trans-DONO</i>					
$\nu(\text{OH})/\nu(\text{OD})$	3572.1			3789	-9		2635.0			2759	-7	
	3568.1						2638.1					
$\nu(\text{N}=\text{O})$	1689.1	1707.8	+19	1644	+55		1682.6	1708.6	+26	1633	+62	
	1688.0						1681.6	1707.5				
$\delta(\text{NOH})/\delta(\text{NOD})$	1265.8	1231.5	-35	1291	-58		1013.9	970.2	-43	1022	-49	
	1263.9	1227.9					1011.4					
$\nu(\text{N}-\text{O})$	800.4			794	-72		748.9			741	-82	
	796.6						744.3					
$\delta(\text{ONO})$	608.7			583	-165		602.4			576	-159	
							601.5					
$\tau(\text{OH})/\tau(\text{OD})$	549.4			582	-56					440	-32	
	548.2											

$\text{CH}_2\text{NOH}$ . In addition, in the  $I_{\text{HF}}$  complex the second much weaker  $\text{O}-\text{H} \cdots \text{N}$  bond is formed between the  $\text{O}-\text{H}$  group of  $\text{CH}_2\text{NOH}$  and the nitrogen atom of HONO. The second interaction is reflected in much stronger perturbation of the NOH group vibrations of formaldoxime in the  $I_{\text{HF}}$  complex than in

the  $II_{\text{HF}}$  one. In Table 2 the observed frequency shifts of the  $I_A$  bands with respect to the corresponding bands of  $\text{CH}_2\text{NOH}$  and *trans-HONO* monomers ( $\Delta\nu_{\text{exp}} = \nu_{\text{com}} - \nu_{\text{mon}}$ ) are compared with the calculated shifts for the  $I_{\text{HF}}$  and  $II_{\text{HF}}$  complexes. As one can see there is good agreement between the observed

frequency shifts and the calculated ones for the  $I_{HF}$  complex. This fact indicates that the  $I_A$  bands correspond to the  $CH_2NOH \cdots trans\text{-HONO}$  complex of structure  $I_{HF}$ .

The most informative on the structure of the  $CH_2NOH \cdots trans\text{-HONO}$  complex, characterized by the  $I_B$  group of bands, are the two absorptions at  $1707.8\text{ cm}^{-1}$  and at  $1231.5, 1227.9\text{ cm}^{-1}$  corresponding to the perturbed  $\nu(N=O)$  and  $\delta(NOH)$  vibrations of *trans*-HONO. The  $N=O$  stretch is shifted toward higher frequencies and the  $NOH$  bend toward lower ones with respect to the corresponding *trans*-HONO vibrations. The earlier studies of HONO complexes with HCl and HF showed that such perturbation of HONO vibrations is characteristic for the structures in which the oxygen atom of HONO serves as a proton acceptor for a proton donor.<sup>20</sup> Among the optimized  $CH_2NOH \cdots trans\text{-HONO}$  structures the  $V_{HF}$  is the only one in which OH of *trans*-HONO acts as a proton acceptor for the OH group of formaldoxime. In Table 3 the experimental frequency shifts of the identified vibrations are compared with those calculated for the  $V_{HF}$  structure. There is reasonable agreement between the observed and calculated frequency shifts for both the identified  $CH_2NOH$  and HONO vibrations. In particular, the observed perturbations of the three identified  $NOH$  group vibrations of formaldoxime show very good agreement with the calculated shifts. So, we may assign with confidence the  $I_B$  group of bands to the  $V_{HF}$  structure.

The fact that in matrices there is present the most stable complex  $I_{HF}$  and one of the complexes corresponding to local minima, namely  $V_{HF}$ , indicates that the formation of the complexes is controlled not only by thermodynamics but also by the kinetics. The formation of the particular structure may be controlled by the initial orientation of the two interacting molecules. Once the structure corresponding to one of the local minima is formed, it may be stabilized in the matrix if the energy barrier corresponding to its conversion to another local structure or to the global minimum is larger than the system energy.

**Photochemistry of the  $CH_2NOH \cdots trans\text{-HONO}$  Complexes. Identification of the Photoproducts.** The  $CH_2NOH/HONO(DONO)/Ar$  matrices were subjected to  $\lambda > 345\text{ nm}$  irradiation and to the full output of the mercury lamp. The photochemistry of HONO in argon and nitrogen matrices has been reported earlier.<sup>21,22</sup> Nitrous acid trapped in solid argon or nitrogen and subjected to  $\lambda > 345\text{ nm}$  radiation photodissociates into OH and NO radicals. The secondary reactions lead to the formation of  $NO_2$ ,  $N_2O_3$  and  $H_2O$  products. The concentration of the secondary reactions products increases with an increase of HONO concentration in the matrix.

When the  $CH_2NOH/HONO/Ar$  matrix is subjected to  $\lambda > 345\text{ nm}$  radiation, the  $I_A$  and  $I_B$  bands of the  $CH_2NOH \cdots trans\text{-HONO}$  complexes gradually diminish, and, in addition, the bands due to HONO monomers also slightly diminish. In the spectra recorded after photolysis, the bands characteristic for the primary and secondary HONO photolysis products appear and, additionally, a set of new bands is observed characteristic for the products of the photochemical reactions that undergo the  $CH_2NOH \cdots trans\text{-HONO}$  complexes. All the main photoproducts discussed in this paper are formed when the matrix is subjected to  $\lambda > 345\text{ nm}$  irradiation. The irradiation with the full output of the Hg lamp just helped us to assign the new bands to different photoreaction products. The new bands are separated into three groups, marked by  $I_{FN}$ ,  $I_{FNW}$  and  $II_{FNW}$ , on the basis of their behavior in all performed experiments. The bands belonging to particular group,  $I_{FN}$ ,  $I_{FNW}$  or  $II_{FNW}$ , have the same relative intensities in all performed experiments. The relative intensities of the  $I_{FN}$ ,  $I_{FNW}$  and  $II_{FNW}$  bands vary slightly

in experiments with  $\lambda > 345\text{ nm}$  radiation. Moreover, the relative intensities of the  $I_{FN}$ ,  $II_{FNW}$  bands increase with respect to the  $I_{FNW}$  ones in experiments in which the matrix is irradiated with the full output of Hg lamp. However, in all performed experiments the  $I_{FNW}$  bands are much more intense than the bands of the other two groups,  $I_{FN}$  and  $II_{FNW}$ . The frequencies of the bands assigned to the three groups are presented in Table 4. The corresponding bands of the  $I_{FN}$ ,  $I_{FNW}$  and  $II_{FNW}$  groups were also observed in the experiments with  $CH_2NOH/DONO/Ar$  matrices and their frequencies are also collected in Table 4. In Figures 2 and 3 curves (b) present the spectra of the  $CH_2NOH/HONO/Ar$  and  $CH_2NOH/DONO/Ar$  matrices recorded after photolysis.

As one can see in Table 4 all three groups,  $I_{FN}$ ,  $I_{FNW}$  and  $II_{FNW}$ , involve three bands that appear in the same frequency regions. The two strongest bands occur in the  $1720\text{--}1697\text{ cm}^{-1}$  and  $744\text{--}736\text{ cm}^{-1}$  regions, respectively, and the weaker one in the  $993\text{--}958\text{ cm}^{-1}$  region for all three groups. This fact suggests that the three groups correspond to one species possibly perturbed by the interaction with another molecule (or molecules) present in the matrix. Moreover, each group contains a band that appears in the region of the water stretching vibration suggesting that water may be also a photoreaction product. One has to remember, however, that water may be a secondary product of HONO photodissociation, as it is formed in recombination reaction of OH radicals. Two facts evidence that water is a photochemistry product of the  $CH_2NOH \cdots trans\text{-HONO}$  complex. First, the bands appearing in the region of the water stretching vibrations and belonging to  $I_{FNW}$ ,  $II_{FNW}$  groups are quite strongly perturbed and they do not appear in the spectra of photolyzed HONO/Ar matrix. Second, in the experiment with DONO the bands due to HDO vibrations are identified. The deposited nitrous acid was deuterated in ca. 90%, so, one may expect that HDO is formed in reaction of OD radicals with  $CH_2NOH$ .

As discussed in the Introduction, Kliegmann and Barnes<sup>3</sup> suggested that the reaction between oxime and nitrous acid in solution may lead to the formation of iminoxyl radical, NO, and  $H_2O$  when is performed under certain conditions. One can expect that in the matrix environment iminoxyl radical reacts with NO trapped in the same cage leading to the formation of formaldoxime nitrite. The two molecules, formaldoxime nitrite and water, being trapped in the same cage may interact with each other forming a complex.

**Formaldoxime Nitrite and Its Complexes with Water.** No oxime nitrite molecule has been identified so far, so, we optimized the structure of formaldoxime nitrite (FN) and its two most stable hydrogen bonded complexes in which water is attached to the nitrogen or to the bridge oxygen atom of formaldoxime nitrite (FNW1 and FNW2). The optimized structures of the most stable formaldoxime nitrite isomer and its complexes with water are shown in Figure 4.

Although the MP2 results obtained for formaldoxime nitrite and its complexes with water seemed reasonable, we encountered a singlet–triplet instability of the reference Hartree–Fock wave function indicating that the molecule may share some diradical character. Nontrivial electronic state is probably a result of unusual net of NONO bonds and is also reflected in relatively long  $O_5\text{--}N_6$  distance.

As it is difficult to assess how this effect burdens the MP2 results, we compared them with the ones obtained with a much more elaborate method, namely quadratic configuration interaction<sup>17</sup> with single and double substitutions. Not only does this method work relatively well for more complicated electronic

**TABLE 4: The Observed and Calculated Frequencies (cm<sup>-1</sup>) for Formaldoxime Nitrite (I<sub>FN</sub>) and Its Complexes with H<sub>2</sub>O and HDO (I<sub>FNW</sub>, II<sub>FNW</sub>)<sup>a</sup>**

approx description	exptl						calcd <sup>b</sup>							
	I <sub>FN</sub>		I <sub>FNW</sub>		II <sub>FNW</sub>		FN <sup>d</sup>		FN <sup>e</sup>		FNW1 <sup>e</sup>		FNW2 <sup>e</sup>	
	<i>ν</i> <sub>exp</sub>	<i>I</i> <sup>c</sup>	<i>ν</i> <sub>exp</sub>	<i>I</i>	<i>ν</i> <sub>exp</sub>	<i>I</i>	<i>ν</i> <sub>calc</sub>	<i>I</i>	<i>ν</i> <sub>calc</sub>	<i>I</i>	<i>ν</i> <sub>calc</sub>	<i>I</i>	<i>ν</i> <sub>calc</sub>	<i>I</i>
CH <sub>2</sub> NONO														
<i>ν</i> <sub>as</sub> (CH)							3267	2	3288	1	3290	1	3286	1
<i>ν</i> <sub>s</sub> (CH)							3142	4	3152	4	3154	4	3152	5
<i>ν</i> (N=O)	1697.5	3	1720.1	16	1704.4	2	1763	232	1705	252	1726	291	1713	286
<i>ν</i> (C=N)			1625.9	2			1702	50	1635	53	1638	54	1638	53
<i>δ</i> (CH <sub>2</sub> )	1360.4	0.1	1363.7	0.1			1459	6	1441	8	1445	8	1456	4
<i>ρ</i> (CH <sub>2</sub> )							1233	0	1209	0	1221	1	1219	0
<i>ω</i> (CH <sub>2</sub> )	958.5	0.1	977.4	2	992.1	0.2	1021	32	982	37	996	36	1010	36
<i>ν</i> (NO)							1006	9	958	15	966	17	948	18
<i>ω</i> (NO)							805	0	802	1	809	1	813	1
<i>ν</i> (NO)	740.7	22	743.2	100	736.8	17	814	511	728	451	733	428	721	431
<i>δ</i> (CNO)							627	3	592	3	594	10	599	2
H <sub>2</sub> O														
<i>ν</i> <sub>as</sub> (OH)	3733		3707.2	5	3719.0	0.4			3986	74	3945	117	3953	135
<i>ν</i> <sub>s</sub> (OH)	3638								3865	10	3741	297	3811	98
<i>δ</i> (HOH)									1660	66	1679	22	1661	15
HDO														
<i>ν</i> (OH)	3688		3691.5						3928	46	3930	47	3924	50
<i>ν</i> (OD)	2709		2623.0						2851	21	2731	193	2791	97
<i>δ</i> (HOD)	1398								1455	57	1446	29	1442	30

<sup>a</sup> The relative observed intensities and calculated intensities (km mol<sup>-1</sup>) are also presented. <sup>b</sup> FN, FNW1, FNW2: formaldoxime nitrite monomer (FN) and its two complexes with water (FNW1, FNW2). <sup>c</sup> The relative intensities were measured with respect to the most intense *ν*(NO) band. <sup>d</sup> Calculated by the help of the QCISD(full)/6-311++G(2d,2p) method. <sup>e</sup> Calculated by the help of the MP2/6-311++G(2d,2p) method.

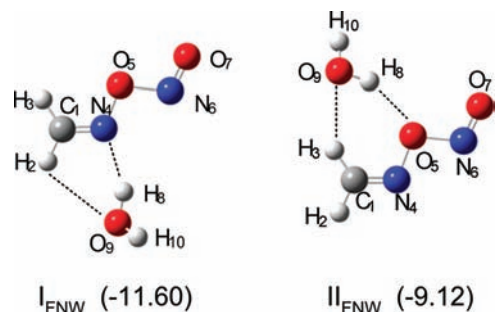


**Figure 4.** Two structures of the complex between the most stable formaldoxime nitrite isomer and water optimized at the QCISD(full)/6-311++G(2d, 2p) level.

structures, but it also provides a tool to estimate reliability of single-reference correlation approach in such cases.<sup>18</sup> Q1 diagnostic, which is an analogous to T1 diagnostic for the coupled cluster method, up to 0.02 is considered to be the criterion for the adequacy of single-reference treatment.

The QCISD method showed stability of three conformers for formaldoxime nitrite, and they are presented in Figure 2 in the Supporting Information. Their selected structural parameters and calculated harmonic frequencies are presented in Tables 3 and 4 in the Supporting Information. The most stable formaldoxime nitrite conformer is calculated to have 6.09, 21.84 kJ mol<sup>-1</sup> lower energy, respectively, than the other two conformers. The comparison of the calculated spectra with the observed ones evidenced that the most stable conformer, shown in Figure 2 in the Supporting Information, is formed in the matrix, and in further discussion we refer to this conformer only.

In Table 5 the geometrical parameters for formaldoxime nitrite calculated using QCISD are compared with those obtained by MP2. As one can see the QCISD parameters are very close to the values from MP2 calculations. The largest difference, as might be expected, is in the case of the O<sub>5</sub>–N<sub>6</sub> bond length.

**TABLE 5: Selected Parameters Describing the Formaldoxime Nitrite, FN, and Its Complexes with Water, FNW1 and FNW2 (Labeling Refers to Figure 4)<sup>a</sup>**

parameter	MP2 <sup>b</sup>	QCISD		
	FN/H <sub>2</sub> O	FN/H <sub>2</sub> O	FNW1	FNW2
<i>r</i> C <sub>1</sub> –H <sub>2</sub>	1.078	1.078	1.078	1.079
<i>r</i> C <sub>1</sub> –H <sub>3</sub>	1.083	1.083	1.082	1.082
<i>r</i> C <sub>1</sub> –N <sub>4</sub>	1.279	1.271	1.271	1.272
<i>r</i> N <sub>4</sub> –O <sub>5</sub>	1.400	1.404	1.400	1.413
<i>r</i> O <sub>5</sub> –N <sub>6</sub>	1.531	1.458	1.459	1.452
<i>r</i> N <sub>6</sub> –O <sub>7</sub>	1.161	1.164	1.164	1.166
<i>r</i> O <sub>9</sub> –H <sub>8</sub>	0.958	0.956	0.961	0.958
<i>r</i> O <sub>9</sub> –H <sub>10</sub>	0.958	0.956	0.955	0.955
<i>R</i> N <sub>4</sub> ···H <sub>8</sub>			2.062	
<i>R</i> O <sub>5</sub> ···H <sub>8</sub>				2.202
<i>R</i> O <sub>9</sub> ···H <sub>3</sub>				2.360
<i>θ</i> C <sub>1</sub> –N <sub>4</sub> –O <sub>5</sub>	110.5	110.1	110.9	109.9
<i>θ</i> N <sub>4</sub> –O <sub>5</sub> –N <sub>6</sub>	104.5	105.9	105.8	106.2
<i>θ</i> O <sub>5</sub> –N <sub>6</sub> –O <sub>7</sub>	109.7	109.5	109.5	109.4
<i>θ</i> N <sub>4</sub> –C <sub>1</sub> –H <sub>2</sub>	115.7	116.1	115.8	115.3
<i>θ</i> N <sub>4</sub> –C <sub>1</sub> –H <sub>3</sub>	122.9	123.0	122.7	123.6
<i>θ</i> H <sub>2</sub> –C <sub>1</sub> –H <sub>3</sub>	121.4	120.8	121.5	121.1
<i>θ</i> H <sub>8</sub> –O <sub>9</sub> –H <sub>10</sub>	104.8	104.6	105.3	105.5
<i>θ</i> N <sub>4</sub> –H <sub>8</sub> –O <sub>9</sub>			149.3	
<i>θ</i> O <sub>5</sub> –H <sub>8</sub> –O <sub>9</sub>				137.0
<i>φ</i> C <sub>1</sub> –N <sub>4</sub> –O <sub>5</sub> –N <sub>6</sub>	180.0	180.0	179.7	179.9
<i>φ</i> N <sub>4</sub> –O <sub>5</sub> –N <sub>6</sub> –O <sub>7</sub>	–180.0	–180.0	179.9	179.9
<i>φ</i> H <sub>2</sub> –C <sub>1</sub> –N <sub>4</sub> –O <sub>5</sub>	–180.0	–180.0	–179.6	–179.9
<i>φ</i> H <sub>3</sub> –C <sub>1</sub> –N <sub>4</sub> –O <sub>5</sub>	0.0	0.0	0.1	0.0
<i>φ</i> O <sub>5</sub> –N <sub>4</sub> –H <sub>8</sub> –O <sub>9</sub>			168.9	
<i>φ</i> N <sub>4</sub> –O <sub>5</sub> –H <sub>8</sub> –O <sub>9</sub>				2.2

<sup>a</sup> Distances are in Å and angles in deg. <sup>b</sup> In calculations by MP2 and QCISD methods the 6-311++G(2d,2p) basis set was applied.

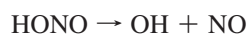
The distance in formaldoxime nitrite calculated on the MP2 level is 1.531 Å, whereas the QCISD method provides a value a bit shorter, namely 1.458 Å. IR spectra calculated using both

methods (Table 4) are qualitatively the same and quantitatively similar. Again, the largest difference is in the case of  $\nu(\text{N}_6\text{O}_5)$ , which is  $728\text{ cm}^{-1}$  (MP2) and  $814\text{ cm}^{-1}$  (QCISD). Q1 diagnostic for this molecule reaches the acceptable value 0.0204, which indicates that the QCISD method provided reliable results and static correlation is not critical. Geometrical parameters for complexes formed by formaldoxime nitrite and water molecule calculated using QCISD (Table 5) and the MP2 method (Table 5 in the Supporting Information) are almost the same apart from the  $\text{O}_5\text{--N}_6$  bond length, which is about  $0.073\text{ \AA}$  longer at the MP2 level. All these results let us assume that the MP2 method can also be used to interpret experimental IR spectra of the complexes. Therefore, in Table 4 for the complexes the IR spectra calculated using only the MP2 method are presented. More precise results need, however, advanced treatment.

In Table 4 the observed frequencies belonging to the  $I_{\text{FN}}$ ,  $I_{\text{FNW}}$  and  $II_{\text{FNW}}$  groups are compared with the calculated harmonic frequencies for formaldoxime nitrite and its two complexes with water.

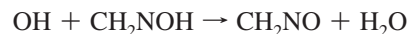
As one may notice, the distinctive feature of the calculated formaldoxime nitrite spectrum is the large intensity of the  $\nu(\text{N=O})$  and  $\nu(\text{N-O})$  stretching vibrations. The absorptions due to the  $\text{N=O}$  and  $\text{N-O}$  stretches are predicted to be ca. 5 times and 9 times more intense than the absorption due to the  $\text{C=N}$  stretching vibration which is the third one with respect to intensity. This is in accord with the experimental spectra observed for the photoproducts characterized by the  $I_{\text{FN}}$ ,  $I_{\text{FNW}}$  and  $II_{\text{FNW}}$  groups of bands. The  $I_{\text{FNW}}$  bands at  $1720.1$ ,  $743.2\text{ cm}^{-1}$  appearing in the  $\text{N=O}$  and  $\text{N-O}$  stretching regions are much more intense than the  $1625.9\text{ cm}^{-1}$  absorption identified for the  $\nu(\text{C=N})$  vibration. The absorptions belonging to the other two groups,  $I_{\text{FN}}$  and  $II_{\text{FNW}}$ , are much weaker but exhibit similar characteristics. Such a spectral characteristic with two bands dominating the spectra is also observed for methyl and propyl nitrites,  $\text{CH}_3\text{ONO}$ <sup>23</sup> and  $\text{C}_3\text{H}_7\text{ONO}$ .<sup>24</sup> The comparison of the experimental frequencies of the  $I_{\text{FN}}$ ,  $II_{\text{FNW}}$  and  $III_{\text{FNW}}$  sets of bands with the frequencies calculated for formaldoxime nitrite and its two complexes with water, FNW1 and FNW2, allows us to identify the reaction photoproducts unambiguously. The most intense among the three groups,  $I_{\text{FNW}}$  bands belong to the more stable FNW1 formaldoxime nitrite complex with water. In turn, the  $I_{\text{FN}}$  bands are due to the formaldoxime nitrite monomer and the  $II_{\text{FNW}}$  ones to the FNW2 complex. Such assignment of the  $I_{\text{FN}}$ ,  $I_{\text{FNW}}$  and  $II_{\text{FNW}}$  bands is in accord with the observed and calculated frequency values of the  $\nu(\text{N=O})$  and  $\nu(\text{N-O})$  stretching vibrations of the three species. The observed frequencies similarly to the calculated ones are increasing in the order  $\nu(\text{N=O})^{I_{\text{FN}}} < \nu(\text{N=O})^{II_{\text{FNW}}} < \nu(\text{N=O})^{I_{\text{FNW}}}$  and  $\nu(\text{N-O})^{II_{\text{FNW}}} < \nu(\text{N-O})^{I_{\text{FN}}} < \nu(\text{N-O})^{I_{\text{FNW}}}$ . From the two identified perturbed water frequencies, the  $\nu(\text{OH})$  corresponding to the stronger FNW1 complex is more perturbed than the  $\nu(\text{OH})$  of the slightly weaker FNW2 complex, as expected. The concentration of the FNW1 complex is much larger than the concentration of the less stable FNW2 complex and the formaldoxime nitrite monomer, FN, as indicated by the relative intensities of the  $\nu(\text{N=O})$  bands corresponding to the three species.

**Reaction Mechanism.** As it is well-known the photodissociation of nitrous acid with radiation  $\lambda > 345\text{ nm}$  leads to the formation of OH and NO radicals with quantum yield close to 1:<sup>25</sup>



The formaldoxime molecule is not affected by this radiation, so the observed products are formed in the reaction of the OH and

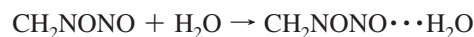
NO radicals with formaldoxime. The reactive OH radical may abstract a hydrogen atom from formaldoxime to produce iminoxyl radical and water molecule:



The formation of HDO in the photochemical reaction of  $\text{CH}_2\text{NOH}$  with DONO evidences that the OD radical abstracts the hydrogen atom from  $\text{CH}_2\text{NOH}$ . The iminoxyl radical thus produced can now react further with NO trapped in the same cage to give formaldoxime nitrite:



The two molecules,  $\text{CH}_2\text{NONO}$  and  $\text{H}_2\text{O}$ , being trapped in the same cage interact with each other and form complexes.



The available literature data and the final products identified in the studied reaction do support the above postulated mechanism of the hydrogen atom abstraction from the OH group of the formaldoxime molecule and not from the  $\text{CH}_2$  one. As stated in the Introduction Kliegman and Barnes<sup>3</sup> postulated such a mechanism for the reaction between oximes and HONO in solutions. Preliminary mechanistic studies of deprotection of oximes to their corresponding carbonyl compounds through the use of electron-transfer reaction also suggest the involvement of an iminoxyl radical as an intermediate.<sup>9</sup> The formation of formaldoxime nitrite in the present study evidences that the reaction of  $\text{CH}_2\text{NOH}$  with OH goes via abstraction of H from OH group of  $\text{CH}_2\text{NOH}$ . The abstraction of hydrogen from the  $\text{CH}_2$  group produces the  $\text{CHNOH}$  radical that is expected to form  $\text{CH}(\text{NO})\text{NOH}$  and not  $\text{CH}_2\text{NONO}$  in reaction with NO. Moreover, our calculations reveal that formation of iminoxyl radical is much more thermodynamically favorable. Two possible isomers of  $\text{CHNOH}$  are  $73.62$  and  $87.55\text{ kJ mol}^{-1}$  less stable than iminoxyl radical.

As reported recently, the OH radical may abstract the hydrogen atom from the OH group of carboxylic acids and alcohols.<sup>26,27</sup> The theoretical studies of the reaction between OH radical and formic acid indicated that the main reaction path occurs via abstraction of the hydrogen atom from the OH group and not from the CH one.<sup>26</sup> The reaction of OH with methanol may also occur via hydrogen abstraction from the OH group.<sup>27</sup>

The infrared spectrum of iminoxyl radical isolated in an argon matrix has been reported.<sup>28</sup> The radical was obtained through transfer of  $\text{CH}_2$  from ketene to NO by photoexcitation of reactants in solid argon. We observed no absorption due to the  $\text{CH}_2\text{NO}$  radical in the studied spectra. This can be explained by a very low concentration (if any) of the radical due to its rapid reaction with NO that is its nearest neighbor enclosed in the same cage.

## Conclusions

The FTIR matrix isolation and MP2/6-311++G(2d,2p) study of the complexes between formaldoxime and nitrous acid indicate that two types of complexes are present in the matrix. The cyclic complex corresponding to a global minimum on PES is stabilized by two  $\text{O-H} \cdots \text{N}$  bonds: a strong one between the OH group of HONO and the nitrogen atom of  $\text{CH}_2\text{NOH}$  and a weak one between OH of formaldoxime and the nitrogen atom of HONO. In the other complex present in the matrix the

OH group of formaldoxime acts as a proton donor toward the OH group of HONO. The products of the photochemical reactions induced by the irradiation ( $\lambda > 345$  nm) of the complexes are formaldoxime nitrite and water. The two molecules being trapped in one cage form two types of complexes with water attached to the nitrogen or bridge oxygen atoms. The intermediate in this reaction is iminoxyl radical that is formed in the abstraction reaction of hydrogen atom from OH group of formaldoxime by OH radical. The iminoxyl radical reacts readily with NO to form formaldoxime nitrite which is identified for the first time. The MP2 and QCISD(full) calculations with the 6-311++G(2d,2p) basis set confirm the identities of the reaction photoproducts.

**Acknowledgment.** The authors gratefully acknowledge a grant of computer time from the Wrocław Center for Networking and Supercomputing.

**Supporting Information Available:** MP2/6-311++G(2d,2p) results for the formaldoxime–nitrous acid complexes. QCISD(full)/6-311++G(2d,2p) and MP2/6-311++G(2d,2p) results for the formaldoxime nitrite conformers. MP2/6-311++G(2d,2p) parameters for the formaldoxime nitrite–water complexes. This material is available free of charge via the Internet at <http://pubs.acs.org>.

## References and Notes

- Manasse, O. *Ber. Dtsch. Chem. Ges.* **1888**, *21*, 2176–2177.
- Claisen, L.; Manasse, O. *Ber. Dtsch. Chem. Ges.* **1889**, *22*, 530–533.
- Kliegman, J. M.; Barnes, R. K. *J. Org. Chem.* **1972**, *37*, 4223–4225.
- Adamopoulos, S.; Boulton, A. J.; Tadayouni, R. *J. Chem. Soc., Perkin Trans. I* **1987**, *207*, 3–2077, and references therein.
- Bandgar, B. P.; Kale, R. R.; Kunde, L. B. *Monatsh. Chem.* **1998**, *129*, 1057–1060.
- Lakouraj, M. M.; Noorian, M.; Mokhtary, M. *React. Funct. Polym.* **2006**, *66*, 910–915.
- Joubert, E.; Courtois, X.; Marecot, P.; Canaff, C.; Duprez, D. *J. Catal.* **2006**, *243*, 252–262.
- Yang, Y.; Zhang, D.; Wu, L.-Z.; Chen, B.; Zhang, L.-P.; Tung, Ch.-H. *J. Org. Chem.* **2004**, *69*, 1788–1791.
- Peter de Lijser, H. J.; Fardoun, F. H.; Sawyer, J. R.; Quant, M. *Org. Lett.* **2002**, *4*, 2325–2328.
- Golec, B.; Mielke, Z. *J. Mol. Struct.* **2007**, *844–845*, 242–249.
- Heikkilä, A.; Pettersson, M.; Lundell, J.; Khriachtchev, L.; Räsänen, M. *J. Phys. Chem. A* **1999**, *103*, 2945–2951.
- Mielke, Z.; Tokhadze, K. G.; Latajka, Z.; Ratajczak, E. *J. Phys. Chem.* **1996**, *100*, 539–545.
- Mielke, Z.; Wierzejewska, M.; Olbert-Majkut, A.; Krajewska, M.; Tokhadze, K. G. *J. Mol. Struct.* **1997**, *436–437*, 339–347.
- Frisch, M. J.; Trucks, G. W.; Schlegel, H. B.; Scuseria, G. E.; Robb, M. A.; Cheesman, J. R.; Montgomery, Jr., J. A.; Vreven, T.; Kudin, K. N.; Burant, J. C.; Millam, J. M.; Iyengar, S. S.; Tomasi, J.; Barone, V.; Mennucci, B.; Cossi, M.; Scalmani, G.; Rega, N.; Petersson, G. A.; Nakatsuji, H.; Hada, M.; Ehara, M.; Toyota, K.; Fukuda, R.; Hasegawa, J.; Ishida, M.; Nakajima, T.; Honda, Y.; Kitao, O.; Nakai, H.; Klene, M.; Li, X.; Knox, J. E.; Hratchian, J. P.; Cross, J. B.; Adamo, C.; Jaramillo, J.; Gomperts, R.; Stratmann, R. E.; Yazyev, O.; Austin, A. J.; Cammi, R.; Pomelli, C.; Ochterski, J. W.; Ayala, P. Y.; Morokuma, K.; Voth, G. A.; Salvador, P.; Dannenberg, J. J.; Zakrzewski, V. G.; Dapprich, S.; Daniels, A. D.; Strain, M. C.; Farkas, O.; Malick, D. K.; Rabuck, A. D.; Raghavachari, K.; Foresman, J. B.; Ortiz, J. V.; Cui, Q.; Baboul, A. G.; Clifford, S.; Cioslowski, J.; Stefanov, B. B.; Liu, G.; Liashenko, A.; Piskorz, P.; Komaromi, I.; Martin, R. L.; Fox, D. J.; Keith, T.; Al-Laham, M. A.; Peng, C. Y.; Nanayakkara, A.; Challacombe, M.; Gill, P. M. W.; Johnson, B.; Chen, W.; Wong, M. W.; Gonzales, C.; Pople, J. A. *GAUSSIAN 03, revision C.02*; Gaussian Inc.: Wallingford, CT, 2004.
- Frisch, M. J.; Pople, J. A.; Binkley, J. S. *J. Chem. Phys.* **1984**, *80*, 3265–3269.
- Krishnan, R.; Binkley, J. S.; Seeger, R.; Pople, J. A. *J. Chem. Phys.* **1980**, *72*, 650–654.
- Pople, J. A.; Head-Gordon, M.; Raghavachari, K. *J. Chem. Phys.* **1987**, *87*, 5968–5975.
- Lee, T. J.; Rendell, A. P.; Taylor, P. R. *J. Phys. Chem.* **1990**, *94*, 5463–5468.
- Boys, S. F.; Bernardi, F. *Mol. Phys.* **1970**, *19*, 553–566.
- Latajka, Z.; Mielke, Z.; Olbert-Majkut, A.; Wiczorek, R.; Tokhadze, K. G. *Phys. Chem. Chem. Phys.* **1999**, *1*, 2441–2448.
- Mielke, Z.; Olbert-Majkut, A.; Tokhadze, K. G. *J. Chem. Phys.* **2003**, *118*, 1364–1377.
- Olbert-Majkut, A. Ph.D. Thesis, University of Wrocław, Poland, 2001.
- Bodenbinder, M.; Ulic, S.; Willner, H. *J. Phys. Chem.* **1994**, *98*, 6441–6444.
- Mátyus, E.; Magyarfalvi, G.; Tarczay, G. *J. Phys. Chem. A* **2007**, *111*, 450–459.
- Cox, R. A.; Derwent, R. G. *J. Photochemistry* **1976/77**, *6*, 23–24.
- Anglada, J. M. *J. Am. Chem. Soc.* **2004**, *126*, 9809–9820.
- Feng, J.; Aki, S. N. V.; Chateaufneuf, J. E.; Brennecke, J. F. *J. Phys. Chem. A* **2003**, *107*, 11043–11048.
- McCluskey, M.; Frei, H. *J. Phys. Chem.* **1993**, *97*, 5204–5207.